

# GUNNEL: Guided Mixup Augmentation and Multi-View Fusion for Aquatic Animal Segmentation

Minh-Quan Le<sup>1,2†</sup>, Trung-Nghia Le<sup>3\*†</sup>, Tam V. Nguyen<sup>4</sup>, Isao Echizen<sup>3</sup>  
and Minh-Triet Tran<sup>1,2,5</sup>

<sup>1</sup>Vietnam National University, Thu Duc City, 700000, Ho Chi Minh, Vietnam.

<sup>2</sup>University of Science, 227 Nguyen Van Cu, District 5, 700000, Ho Chi Minh, Vietnam.

<sup>3</sup>National Institute of Informatics, 2-1-2 Hitotsubashi, Chiyoda-ku, 1018043, Tokyo, Japan.

<sup>4</sup>University of Dayton, 300 College Park, Dayton, 45469, Ohio, US.

<sup>5</sup>John von Neumann Institute, Thu Duc City, 700000, Ho Chi Minh, Vietnam.

\*Corresponding author(s). E-mail(s): [ltnghia@nii.ac.jp](mailto:ltnghia@nii.ac.jp);

Contributing authors: [lmquan@selab.hcmus.edu.vn](mailto:lmquan@selab.hcmus.edu.vn); [tamnguyen@udayton.edu](mailto:tamnguyen@udayton.edu);  
[iechizen@nii.ac.jp](mailto:iechizen@nii.ac.jp); [tmtriet@fit.hcmus.edu.vn](mailto:tmtriet@fit.hcmus.edu.vn);

†These authors contributed equally to this work.

## Abstract

Recent years have witnessed great advances in object segmentation research. In addition to generic objects, aquatic animals have attracted research attention. Deep learning-based methods are widely used for aquatic animal segmentation and have achieved promising performance. However, there is a lack of challenging datasets for benchmarking. In this work, we build a new dataset dubbed “Aquatic Animal Species.” We also devise a novel **GU**ided mixup augme**N**tatio**N** and multi-vi**E**w fusion for aquatic anima**L** segmentation (GUNNEL) that leverages the advantages of multiple view segmentation models to effectively segment aquatic animals and improves the training performance by synthesizing hard samples. Extensive experiments demonstrated the superiority of our proposed framework over existing state-of-the-art instance segmentation methods.

**Keywords:** aquatic animal segmentation, multi-view fusion, guided mixup augmentation, camouflaged animals

## 1 Introduction

Computer vision is an interdisciplinary research field that helps computers gain understanding from visual data sources. The rapid development of deep learning techniques has enabled computer vision applications to become a part of daily life, such as autonomous driving [22], medical treatment [6], entertainment [40], shopping [30], surveillance [29, 39], and wildlife preserve [21].

These applications require the detection and segmentation of various types of objects appearing in images and videos [25, 28].

Animal-related research has recently drawn the attention of the computer vision community. As a result, the number of studies involving animal research using computer vision and deep learning techniques has been increasing, such as measurement of animal behaviors [27] and analysis of animal trajectories [26]. In addition, various

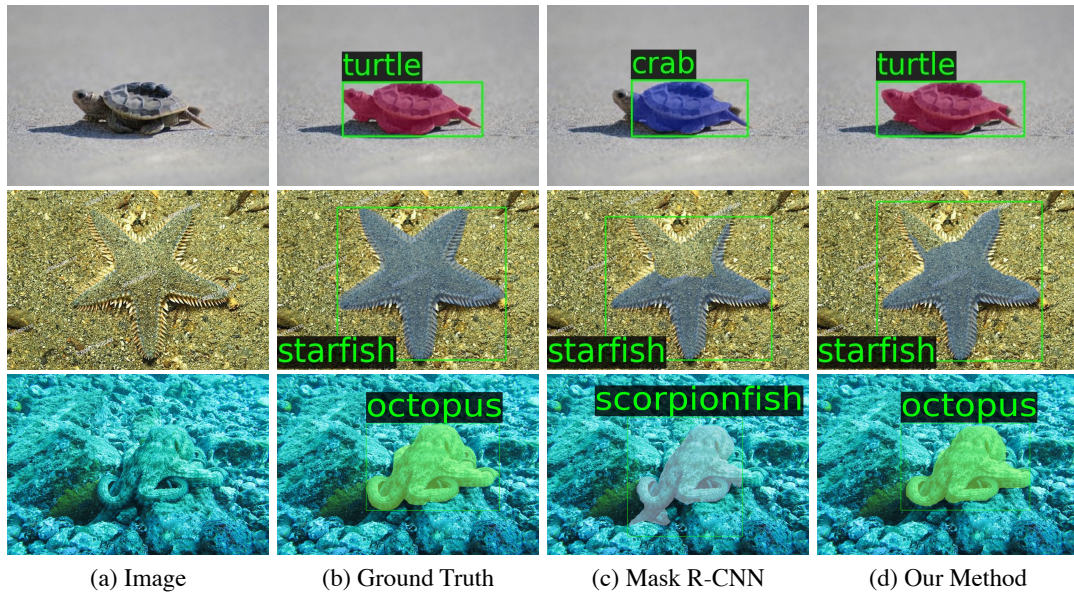


**Fig. 1:** Visual comparison of our method with baseline model. From left to right: input image, overlaid ground truth, Mask RCNN [16], our proposed GUNNEL method.

animal-related datasets have been constructed for specific research purposes [31, 41, 43]. However, there is a lack of research on aquatic animals, especially on automatically localizing and recognizing aquatic animals. We attribute this partially to the lack of appropriate datasets for training, testing, and benchmarking. It has thus become essential to construct datasets of aquatic animals in order to develop methods for aquatic animal instance detection and segmentation.

We created a dataset to encourage more research on aquatic animal segmentation, namely “Aquatic Animal Species (AAS).” Our dataset consists of 4,239 images with 5,041 instances of 46 aquatic animal species. We also devised a simple yet effective **GU**ided mixup augme**N**tatio**N** and multi-**viE**w fusion for aquatic anima**L** segmentation (**GUNNEL**). In our proposed multi-view fusion method, results of multiple single-view segmentation models are fused under the guidance of a mask-agnostic controller. To overcome issues of limited training data, we developed a guided mixup augmentation method based on a confusion matrix to improve training performance. We further established the first comprehensive benchmark for aquatic animal segmentation. Extensive experiments on the newly constructed dataset

demonstrated the superiority of our proposed method over state-of-the-art instance segmentation methods (see Figure 1). The dataset, source code, and trained models will be released with the publication of our paper.

Our contributions are five-fold:

- We present a comprehensive study on aquatic animal segmentation, which is more complicated than general object segmentation. This work is the first exploration of the task of aquatic animal segmentation to the best of our knowledge.
- We propose a new multi-view fusion strategy for aquatic animal segmentation. Our fusion scheme leverages different instance segmentation models by using multi-view mask fusion under the guidance of a mask-independent controller.
- We develop a new guided mixup augmentation method for improving segmentation performance. Our augmentation strategy boosts the performance of deep learning models from a discriminative ability perspective and maintains the global context, especially for camouflaged aquatic animals.
- We construct a new dataset for aquatic animal segmentation. Our newly constructed

AAS dataset contains 4,239 images of 46 aquatic animal species, in which each image has 1.2 instances on average. All images have instance-wise ground truths of the bounding box and segmentation mask.

- We introduce a comprehensive AAS benchmark to support advancements in this research field.

The remainder of this paper is organized as follows. Section 2 summarizes the related work. Next, Section 3 presents our newly constructed AAS dataset. Our proposed GUNNEL framework for aquatic animal segmentation is introduced in Section 4. Section 5 reports the evaluation and in-depth analysis of our proposed method. Finally, Section 6 draws the conclusion and paves the way for future work.

## 2 Related Work

### 2.1 Instance Segmentation

Instance segmentation methods not only localize objects but also predict per-pixel segmentation masks of objects with their corresponding semantic labels. Mask RCNN [16], which is known as a pioneer end-to-end deep neural network for instance segmentation, and its variances (*e.g.*, Cascade Mask RCNN [4], Mask Scoring RCNN [17]) perform detect-then-segment. These models involve object mask segmentation after bounding box object detection by adding segmentation branches on top of Faster RCNN [33]. Cascade Mask RCNN [4, 15] and Mask Scoring RCNN [17] were developed to solve issues of the intersection over union (IoU) threshold by training a multi-stage architecture and evaluating the quality of mask prediction.

More recent efforts have explored instance segmentation using ideas from other computer vision and computer graphics branches [5, 19, 42, 47]. Wang *et al.* [42] designed a universal, lightweight, and highly effective feature upsampling operator. Zhu *et al.* [47] improved the ability to concentrate on pertinent image regions through comprehensive integration of deformable convolutions. Cao *et al.* [5] proposed a global context network by applying query-independent formulation into network layers. Kirillov *et al.* [19] developed a rendering-like segmentation module, which performs point-based segmentation at adaptively

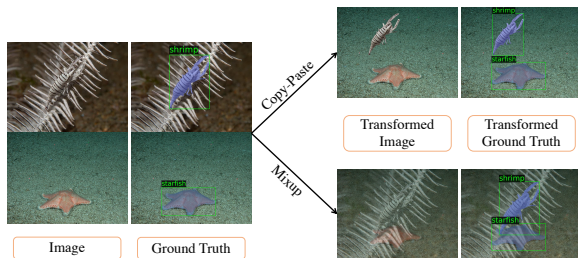


**Fig. 2:** Comparison between copy-paste [12] and mixup [46] data augmentations. Copy-paste method is not helpful because camouflaged aquatic animals become visible while mixup method transforms entire of images, outputting unrealistic results (best viewed online in color with zoom). Our proposed guided mixup augmentation utilizes both approaches to achieve better performance.

selected locations based on an iterative subdivision algorithm. Rossi *et al.* [34] applied non-local building blocks and attention mechanisms to overcome the limitation of RoI extractors. Different normalization layers, such as Group Normalization [44] and Weight Standardization [32], have been proposed for reducing gradient vanishing to improve the training performance.

The fusion of single segmentation models, dubbed ensemble modeling, also plays an important role in improving performance. Indeed, under circumstances when real-time inference is not required, ensemble modeling can improve robustness and effectiveness. Several object detection techniques have been introduced that combine the predictions of multiple models and obtain a final set of detection results. They include non-maximum suppression (NMS) [7, 13], soft-NMS [2], and weighted boxes fusion [36]. To the best of our knowledge, a fusion technique for the instance segmentation task has not been developed. Here, we present a novel fusion algorithm leveraging a simple detector that performs as a view controller to ensemble predictions of instance segmentation models.

### 2.2 Data Augmentation

Data augmentation consists of a collection of transformation techniques that inflates the size and quality of training datasets. These techniques are used to improve the generalization of deep

**Table 1:** Statistics for animal image datasets used in our experiments.

Dataset	#Cat.	#Train Img.	#Test Img.	#Img. per Cat.
MAS3K[23]	37	1,488	1,007	67.4
COD10K (Subset) [10]	21	758	293	50.0
CAMO++ (Subset)[20]	32	366	166	16.6
Collected AAS	46	2,582	1,657	92.1

learning models [35]. Through data augmentation, deep learning models are able to extract additional information from a dataset by data warping or oversampling. Data warping augmentation methods, which include geometric and color transformations, are always used in training deep learning models (*e.g.* scaling, flipping, rotation, random crop [38], color jittering [37]).

On the other hand, oversampling augmentation methods [14, 46] synthesize objects and then integrate them into the original training dataset. Zhang *et al.* [46] proposed mixup augmentation by creating convex combinations of pairs of samples and their labels to train neural networks. Yun *et al.* [45] introduced CutMix mechanism to overcome the model confusion of localization of the mixup method. Bochkovskiy *et al.* [1] developed Mosaic technique by mixing different contextual images to make object detectors conscious of objects outside their usual contexts and smaller scale as well.

In addition, recent object-aware augmentation methods [11, 12] aim to copy objects from an image and paste them into another image. Dvornik *et al.* [8] leveraged segmentation annotations and modeled visual context surrounding objects to place copied objects. Fang *et al.* [11] explored a location probability map and found places having similar local appearances to place randomly jittered objects. Dwibedi *et al.* [9] proposed to cut objects and paste them into diverse background scenes. Ghiasi *et al.* [12] constructed a simple copy-paste mechanism by randomly selecting a subset of objects from images and pasting them onto others.

However, existing data augmentation methods do not work well on images of aquatic animals. Aquatic animal images in our AAS dataset contain both camouflaged and non-camouflaged animals. This makes the localization and recognition of an aquatic animal much more complex than animals in other datasets. In addition, identifying

a camouflaged aquatic animal strongly depends on the entire background. This means that simply placing a cloned camouflaged aquatic animal on a random background does not work. Indeed, within different contexts of scenes, the camouflaged aquatic animal becomes far easier to be recognized [21] (see Figure 2).

Our proposed guided mixup augmentation method overcomes this limitation better than existing augmentation methods for three reasons. (1) Rather than two images being randomly chosen and blended, a confusion matrix is leveraged with the aim of guiding the model to concentrate on misclassified categories. (2) The augmentation strategy helps instance segmentation models improve their discriminative ability by choosing instances that belong to strongly confusing categories of the image. (3) Guided mixup augmentation helps preserve the global context for both camouflaged and non-camouflaged aquatic animals.

### 3 Aquatic Animal Species Dataset

To the best of our knowledge, only three currently available animal datasets can be used for aquatic animal segmentation: subsets of the MAS3K [23], COD10K [10], and CAMO++ [20] datasets. However, these datasets have different ranges of categories and a small number of images. This may lead to overfitting when training deep neural networks due to the small number of images in each category (see Table 1).

Our goal is to build a comprehensive benchmark that can be used to evaluate deep learning models. To reach this goal, we reorganized a new dataset by sampling the three datasets noted above and relabeling the sampled images. We first selected images containing aquatic animals from these datasets. Next, we manually discarded duplicate selected images and relabeled the images

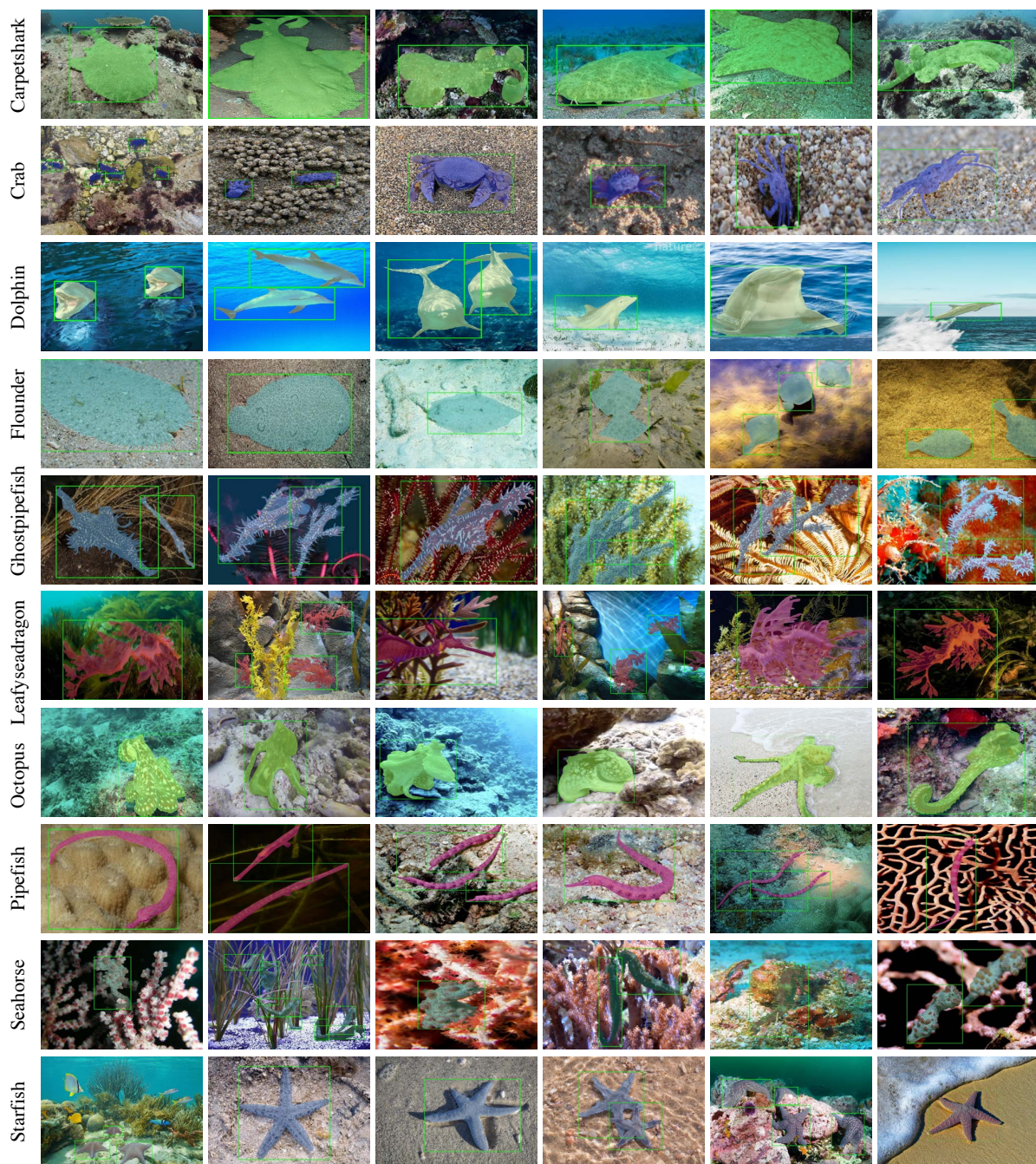


**Fig. 3:** Visualization of annotated images in our AAS dataset. The ground truth masks are overlaid onto the aquatic animal images.

retained to match the categories in our dataset. Examples of annotated instances in our collected AAS dataset can be viewed in Figure 3.

Our newly constructed Aquatic Animal Species (AAS) dataset contains 4,239 images of aquatic animals in 46 categories. There are 5,041 instances in our dataset, and each image has

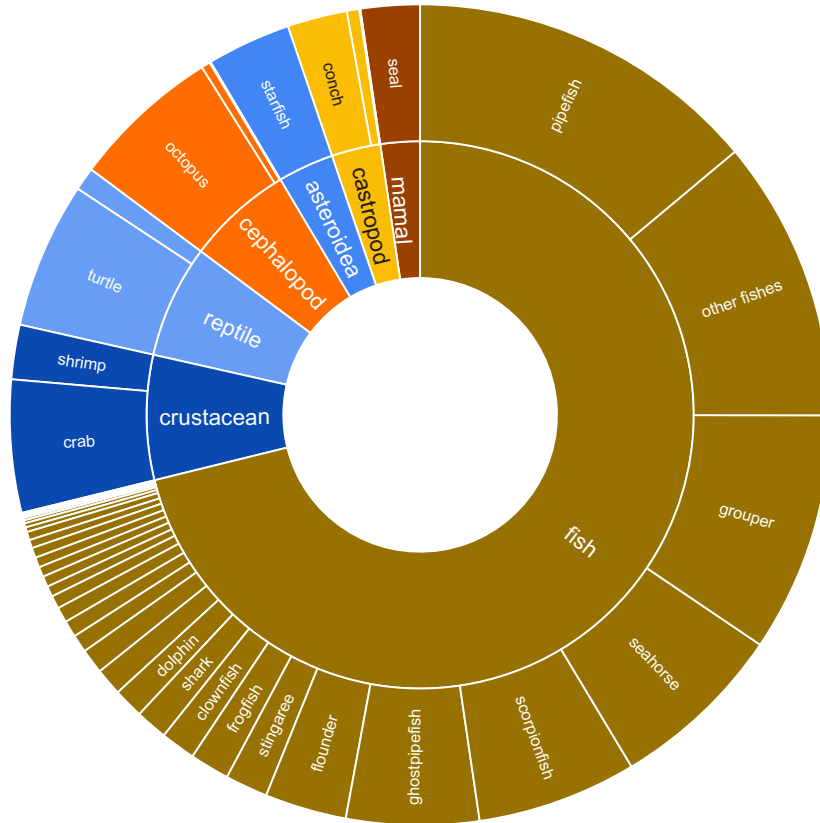


**Fig. 4:** Aquatic animal categories in our AAS dataset (best viewed online in color with zoom). For clear presentation, we do not visualize categories with small number of images.

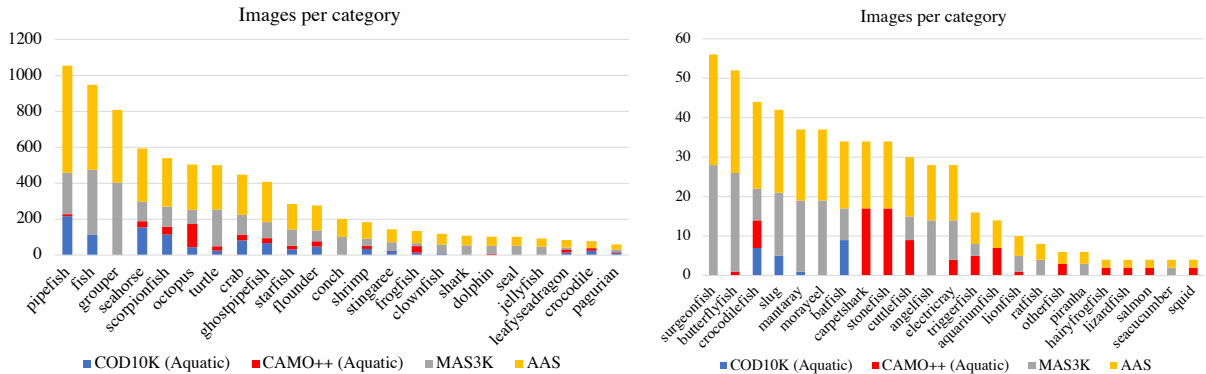


**Fig. 5:** Number of images per category in our AAS, COD10K (Subset), CAMO++ (Subset) and MAS3K datasets.

1.2 instances on average and a maximum of 22 instances. Table 1 shows the overall statistics for our AAS dataset compared with existing datasets. Figure 4 illustrates animal categories in our AAS

dataset. Fish takes the largest ratio with 33 species and 71% number of images. Non-fish animals include 12 species taking 29% number of images.

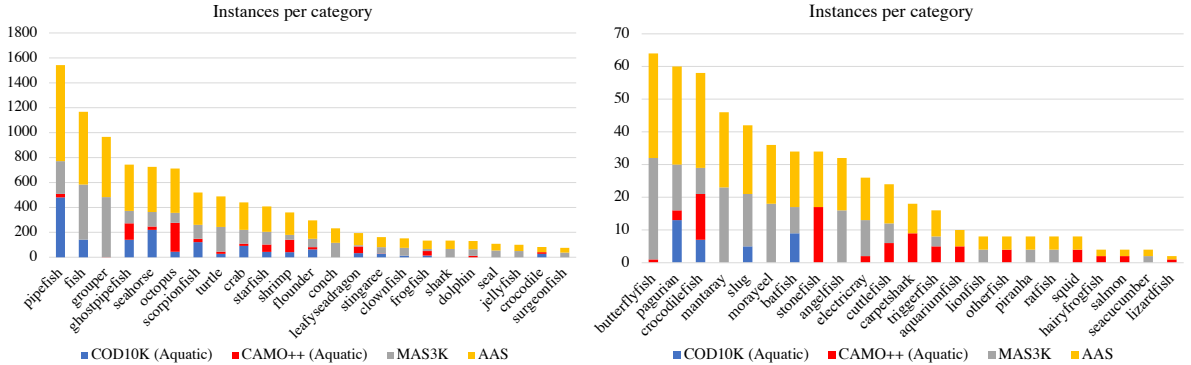


**Fig. 6:** Number of annotated instances per category in our AAS, COD10K (Subset), CAMO++ (Subset) and MAS3K dataset.

The number of images and instances per category are illustrated in Figures 5 and 6, respectively. Our collected AAS dataset has more aquatic categories than CAMO++, COD10K, and MAS3K datasets. Furthermore, with respect to most of the categories, our proposed AAS has more images and instances than those prior datasets.

## 4 Proposed Method

### 4.1 Overview

Instance segmentation methods [16, 17] are imperfect in the sense that each method may have advantages in specific contexts but disadvantages in others. To utilize the strength of different methods, we derived a simple yet efficient **G**UIded mixup augmeNtation and multi-viEw fusion for aquatic animaL segmentation (GUNNEL) to instruct the training procedure and leverage various models through mining image contexts.

Figure 7 illustrates the training stage of our proposed GUNNEL framework. In this stage, instance segmentation models dubbed “single-view models” and a detection model dubbed the “view controller” are trained separately. The object detection-based view controller is trained with two-loss components, including classification and localization losses.

$$\mathcal{L} = \mathcal{L}_{\text{cls}} + \mathcal{L}_{\text{box}} \quad (1)$$

Likewise, single-view instance segmentation is trained with multi-task loss function combining

the loss of classification, localization and segmentation.

$$\mathcal{L} = \mathcal{L}_{\text{cls}} + \mathcal{L}_{\text{box}} + \mathcal{L}_{\text{mask}} \quad (2)$$

The single-view models exploit different contexts to create different segmentation masks for the aquatic animals in the image. The view controller is aimed at producing pseudo bounding box ground truths for fusing multiple single-view models (see Section 4.2).

As shown in Figure 8, in the inference stage, given an unlabeled image, the view controller extracts bounding boxes with high confidence scores from each image. These boxes guide the view controller to fuse the results from single-view models, resulting in the final segmentation mask results.

### 4.2 Multi-View Fusion

Our proposed multi-view mask fusion algorithm uses a mask-independent detector as the guidance view controller. The YOLOv5 [18] model is used as the view controller thanks to its fast training and focusing on both spatial and discriminative representation.

Algorithm 1 illustrates our proposed multi-view fusion algorithm, which receives pseudo bounding box ground truths and segmentation masks from single-view models as input and generates final mask results. It iterates over the images to update a “waiting list.” At each iteration, the segmentation masks of the single-view models for an image are added to the waiting list, and an evaluation is performed to choose the best results.

In particular, when the algorithm is working with the  $i^{\text{th}}$  image, the “result list” contains the

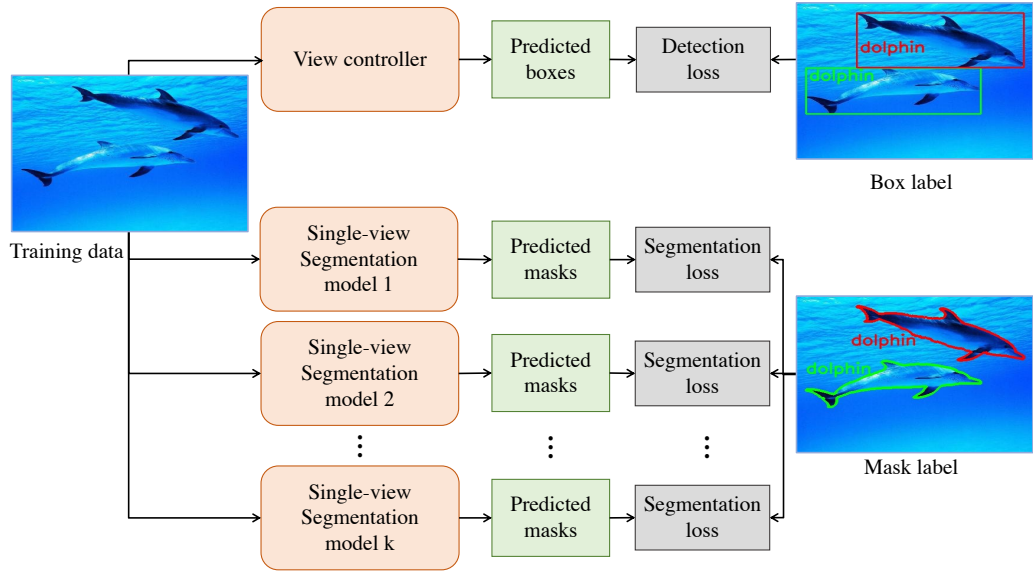


**Fig. 7:** The training stage of our multi-view fusion method (best viewed online in color with zoom).

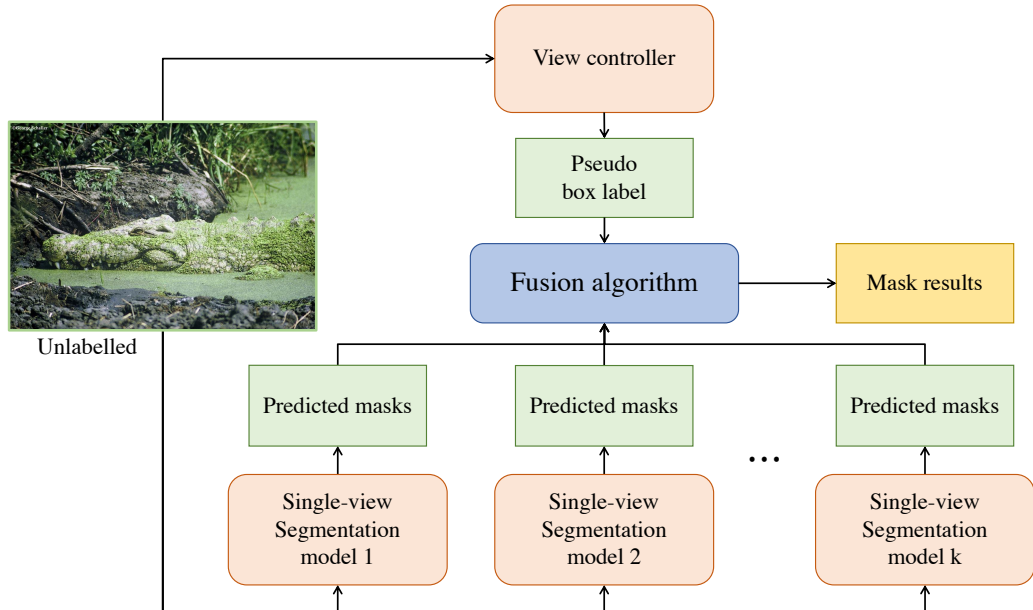


**Fig. 8:** The inference stage of our multi-view fusion method (best viewed online in color with zoom).

segmentation masks for the first  $i - 1$  images. The waiting list is the union of the result list and a temporary segmentation mask for the  $i^{th}$  image. The Average Precision (AP) between the pseudo ground truths and the waiting list is then evaluated. If the  $n^{th}$  segmentation model provides the

highest AP value, its segmentation mask for the  $i^{th}$  image is appended to the result list.

### 4.3 Guided Mixup Augmentation

Aquatic animals involve both camouflaged and non-camouflaged ones, confusing deep learning



**Algorithm 1** Multi-view fusion algorithm.**Input:**

1. Collection of instance segmentation results  $\text{ins}[N \times K]$  for  $K$  single-view models on  $N$  images.
2. List of pseudo ground truths  $\text{pseudo}_{\text{box}}[N]$  for  $N$  images from view controller.

**Output:** List of results  $\text{res}[N]$  for  $N$  images. Each element of  $\text{ins}$ ,  $\text{res}$  contains all segmented results of corresponding image.

- 1:  $\text{res} \leftarrow \emptyset$
- 2: **for**  $i \leftarrow 1$  to  $N$  **do**
- 3:  $\hat{k} \leftarrow \underset{k \in K}{\text{argmax}}(\mathbf{AP}(\text{pseudo}_{\text{box}}[1 : i], \text{res} \cup \text{ins}[i, k]))$
- 4:  $\text{res} \leftarrow \text{res} \cup \text{ins}[i, \hat{k}]$
- 5: **end for**
- 6: **return**  $\text{res}$

models (see Section 2.2). To address this problem, we developed a training procedure using guided mixup augmentation for instance segmentation. Different from the mixup augmentation method [46], which chooses random pairs of images for blending, our wisely guided mixing strategy selects images using a confusion matrix. Figure 9 shows the workflow of our proposed guided mixup augmentation, which involves two stages: warmup learning and augmentation learning.

The first few steps are for warmup learning: the single-view model (*i.e.*, the instance segmentation model) tries to learn and adapt to new data by learning from only original images. Therefore, data augmentation is not used in these initial learning steps.

Next, in the augmentation learning stage, when the single-view model achieves stable weights at the end of each epoch, a confusion matrix is constructed based on the bounding box IoU (intersection over union) between the segmentation results and ground truths. For each segmented instance, all instance ground truths having an IoU with the segmented instance mask larger than the threshold  $\alpha = 0.5$  are selected. The category and classification score for all matching pairs of results and ground truths are extracted and used to create guided confusion matrix ( $C$ ) for the next epoch.

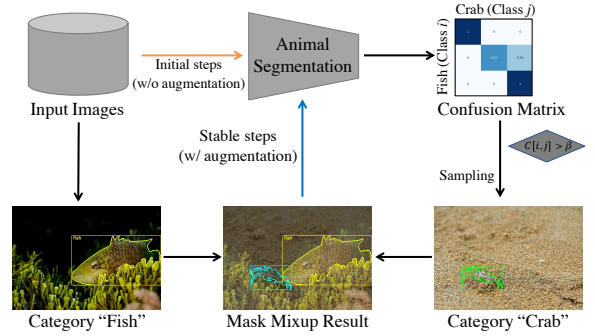


**Fig. 9:** Workflow of proposed guided mixup augmentation using confusion matrix (best viewed online in color with zoom).

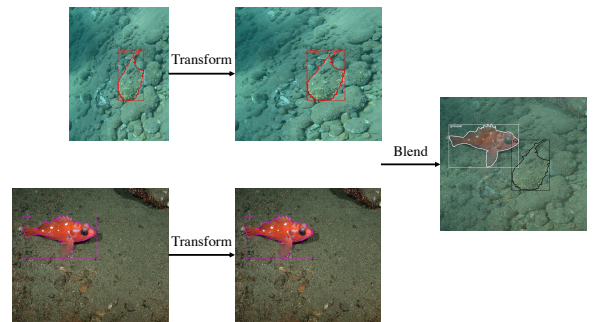


**Fig. 10:** Blending process for data augmentation (best viewed online in color with zoom).

In the next epoch, given an input image, we select an ambiguous image from the training set for mixing. In particular, for pairs of strongly misclassified categories  $(i, j)$  (*i.e.*,  $C[i][j]$  is larger than the threshold  $\beta = 0.2$ ), if the input image contain instances of category  $i$ , a random image having instances in category  $j$  is selected from the training set.

Figure 10 illustrates our blending strategy. Given two images  $a$  and  $b$  with resolutions  $(H_1, W_1)$  and  $(H_2, W_2)$ , we randomly resize the images within the range  $(\frac{H_1+H_2}{2} \times [0.4, 0.6], \frac{W_1+W_2}{2} \times [0.4, 0.6])$  and then mix them together using  $c = \gamma \times \phi(a) + (1 - \gamma) \times \phi(b)$ , where  $\phi(\cdot)$  denotes random cropping and translation operations. Output image  $c$  contains all instances in both original images along with their ambiguous categories. Standard transformations, such as color jitter, brightness adjustment, and horizontal flipping, are applied to the output image. We empirically set  $\gamma = 0.5$ .

**Table 2:** Average Precision results of state-of-the-art instance segmentation methods and the proposed method; 1<sup>st</sup> and 2<sup>nd</sup> places are shown in **blue** and **red**, respectively.

Method	AP	AP50	AP75
Mask RCNN [16]	15.6	24.3	15.8
Cascade Mask RCNN [4]	20.6	30.2	22.2
GN-Mask RCNN [44]	15.5	23.2	16.3
Mask Scoring RCNN [17]	17.3	27.1	18.1
Deformable ConvNets [47]	16.0	24.0	17.4
GCNet [5]	12.1	18.7	13.0
CARAFE [42]	14.7	22.7	15.2
WS-Mask RCNN [32]	18.7	27.1	20.7
PointRend [19]	12.7	18.7	13.3
GRoIE [34]	17.8	26.8	18.9
Our GUNNEL (Multi-view fusion)	<b>24.9</b>	<b>36.3</b>	<b>26.5</b>
Our GUNNEL (Multi-view fusion + Guided mixup augmentation)	<b>28.3</b>	<b>40.7</b>	<b>31.4</b>

## 5 Experiments

### 5.1 Implementation

We used 10 instance segmentation models as the single-view models in our proposed GUNNEL framework: Mask RCNN [16], Cascade Mask RCNN [4], GN-Mask RCNN [44], Mask Scoring RCNN [17], Deformable ConvNets [47], GCNet [5], CARAFE [42], WS-Mask RCNN [32], PointRend [19], and GRoIE [34]. All of them were employed with the widely used ResNet50-FPN backbone. In addition, YOLOv5 [18] detector was used as the view controller.

All models were trained with a batch size of 2 on an RTX 2080Ti GPU. They were fine-tuned from their publicly released MS-COCO [24] pre-trained models.

The single-view segmentation models were trained using stochastic gradient descent (SGD) optimization [3] with a weight decay of  $10^{-4}$  and momentum of 0.9. The first 500 steps were used for warmup learning, in which the learning rate was set to  $2 \times 10^{-5}$  and then linearly increased to 0.02. The models were then trained for 12 epochs with a base learning rate of 0.02, which was decreased by 10 times at the 8<sup>th</sup> and 11<sup>th</sup> epochs. Data augmentation was not applied in the first epoch so that the models could adapt to the aquatic animal images. From the second epoch, our proposed guided mixup augmentation method was applied. The augmented and original image ratio was kept at 50/50 using a Bernoulli distribution.

The view controller was trained for 500 epochs with an image size of  $1280 \times 1280$ , using default released parameters and our guided mixup data augmentation.

### 5.2 Benchmarking

In this section, we compare our GUNNEL framework with state-of-the-art methods to demonstrate the superiority of the proposed framework.

Table 2 shows the performance of different methods in terms of Average Precision (AP). As can be seen, our proposed GUNNEL achieved the best performance. Even without using data augmentation, our method, which achieved AP of 24.9%, still surpassed the state-of-the-art methods by a remarkable margin in all three AP metrics. Meanwhile, the completed GUNNEL achieved AP of 28.3% and significantly outperformed all compared methods in all metrics. Furthermore, it shows the effectiveness of the proposed guided mixup augmentation, which results in an impressive increase by 13.7%.

Figure 11 shows a visual comparison of compared methods. Our GUNNEL achieved the best results close to the ground truth. Our method effectively handled both segmentation masks and classification labels.

### 5.3 Ablation Study

In this section, we analyze core modules of the proposed GUNNEL framework to verify the effectiveness of each part. In particular, we took into



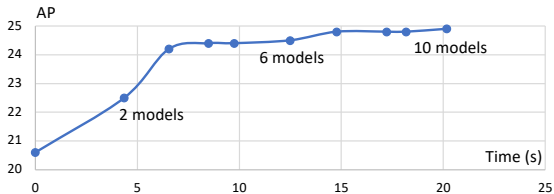
**Fig. 11:** Comparison of results of instance segmentation methods. From left to right: original image is followed by overlaid ground truth and results of our GUNNEL framework, Mask RCNN [16], Cascade Mask RCNN [4], MS RCNN [17], PointRend [19], WS-Mask RCNN [32], GRoIE [34]. Instances shown in color differently from the ground truth denote misclassification. Best viewed in color with zoom.

account the effectiveness of guided mixup augmentation. We also investigated the number of

single-view models and analyzed the complexity of our multi-view fusion algorithm.

**Table 3:** Effectiveness of data augmentation. Best results are shown in blue.

Method	AP	AP50	AP75
None	21.7	32.5	22.5
Random mixup[46]	21.2	31.4	22.7
Instaboost [11]	21.5	31.7	23.9
Copy-paste[12]	22.8	34.0	24.2
Our guided mixup	<b>23.8</b>	<b>34.5</b>	<b>26.7</b>

**Fig. 12:** Trade-off between accuracy and processing time as number of single-view models was increased. Accuracy plateaued at 10 models.

### 5.3.1 Effectiveness of Guided Mixup Augmentation

We demonstrated the usefulness of our proposed guided mixup augmentation method, with its category discrimination ability, by comparing its performance with that of other data augmentation methods, including random mixup [46], instaboost [11], and copy-paste [12]. We used public source codes of data augmentation methods released by the authors. We remark that due to limitations of existing data augmentation methods, we used an ecological version of our GUNNEL with two single-view models (*e.g.* Mask RCNN [16] and Cascade Mask RCNN [4]) in order to conduct the experiment efficiently.

As shown in Table 3, our guided mixup augmentation substantially improved the performance of the GUNNEL framework by 9.7%. The performance of our proposed data augmentation method also surpassed that of existing data augmentation methods by a remarkable margin. Hence, our proposed guided mixup augmentation method can substantially contribute not only to reducing data labeling hours but also to efficiency (*i.e.*, the processing time) and effectiveness (*i.e.*, the performance improvement).

### 5.3.2 Number of Single-View Models

We investigated the effectiveness of our multi-view fusion by increasing the number of single-view models one by one. To show the actual contribution of the proposed fusion algorithm, we did not use our guided mixup data augmentation in the experiments. As shown in Fig. 12, the accuracy of the GUNNEL plateaued at 10 models. Further increases in the number of single-view models would only lead to increased processing time without improving the performance. Hence, we use 10 single-view models in our GUNNEL framework.

### 5.3.3 Complexity of Multi-View Fusion

In this section, we provide the analysis of both the space and time complexity of our multi-view fusion algorithm. As described in Section 4.2, the multi-view fusion algorithm receives a pseudo bounding box from the view controller and predictions of  $N$  images from  $K$  single-view models. However, the excessive increase in the number of single-view models does not result in significant improvement in fusion efficiency and effectiveness. Indeed, Figure 12 illustrates that the fusion results tend to saturate when the number of single-view models rises to 7, and it becomes plateauing at 10 models. On the other hand, inference time grows significantly. That is why we consider the number of single-view models as constant and focus on analyzing the complexity of the fusion algorithm based on the number of images.

To begin with, we explore the time complexity of the multi-view fusion algorithm being dependent on the number of images. The main operator of the fusion algorithm is the AP evaluation inside the loop over  $N$  images. The evaluation procedure of  $i^{th}$  image also relies on  $i - 1$  previous ones. In particular, we calculate the number of evaluation operators,  $n_{op}$ , as the quantities of images

increase:

$$n_{op} = 1 + 2 + \dots + n = \frac{n(n+1)}{2} \in \mathcal{O}(n^2),$$

where  $n$  is the number of total images in the test dataset. As a result, we conclude that the time complexity of the multi-view fusion algorithm is  $\mathcal{O}(n^2)$ .

Likewise, we further peruse the space complexity of the proposed multi-view fusion algorithm. In fact, the space resources expand linearly, corresponding to the number of images. The algorithm particularly takes up the space of  $n$ , multiplying the space of predictions on a single image, where  $n$  is the number of total images. In short, the time complexity and the space complexity of our multi-view fusion algorithm are  $\mathcal{O}(n^2)$  and  $\mathcal{O}(n)$ , respectively.

## 6 Conclusion

This paper investigated the interesting yet challenging problem of aquatic animal segmentation. We created the Aquatic Animal Species (AAS) dataset containing diverse aquatic animal species images. Each image has annotated instance-level mask ground truths. We also developed a novel multi-view fusion algorithm to leverage different instance segmentation models. We further boosted the performance of aquatic animal segmentation by developing a guided mixup augmentation method. Extensive experiments demonstrated that our proposed method achieves state-of-the-art performance on our newly constructed dataset. We expect our AAS dataset to greatly support research activities that automatically identify new aquatic animal species.

We plan to investigate various factors of the given problem in the future. In particular, we will explore the use of contextual information in detecting and segmenting aquatic camouflaged instances. Actually, there are different animals and plant life that live at varying depths of the sea levels. We also plan to extend our work to dynamic scenes such as those in underwater videos. We intend to investigate the impact of the motion in segmenting aquatic camouflaged instances in videos.

## Acknowledgements

This work was funded by the Vingroup Innovation Foundation (VINIF.2019.DA19), National Science Foundation Grant (NSF#2025234), JSPS KAKENHI Grants (JP16H06302, JP18H04120, JP21H04907, JP20K23355, JP21K18023), and JST CREST Grants (JPMJCR20D3, JPMJCR18A6). We gratefully acknowledge NVIDIA for their support of the GPUs.

## References

- [1] Bochkovskiy, A., Wang, C.Y., Liao, H.: YOLOv4: Optimal speed and accuracy of object detection. ArXiv arXiv:2004.10934 (2020)
- [2] Bodla, N., Singh, B., Chellappa, R., Davis, L.S.: Soft-NMS – improving object detection with one line of code. In: ICCV (2017)
- [3] Bottou, L.: Large-scale machine learning with stochastic gradient descent. In: COMPSTAT (2010)
- [4] Cai, Z., Vasconcelos, N.: Cascade r-cnn: Delving into high quality object detection. In: CVPR (2018)
- [5] Cao, Y., Xu, J., Lin, S., Wei, F., Hu, H.: Gcnet: Non-local networks meet squeeze-excitation networks and beyond. In: ICCV Workshop (2019)
- [6] Sainz de Cea, M.V., Diedrich, K., Bakalo, R., Ness, L., Richmond, D.: Multi-task learning for detection and classification of cancer in screening mammography. In: International Conference on Medical Image Computing and Computer-Assisted Intervention. pp. 241–250 (2020)
- [7] Dalal, N., Triggs, B.: Histograms of oriented gradients for human detection. In: CVPR (2005)
- [8] Dvornik, N., Mairal, J., Schmid, C.: Modeling visual context is key to augmenting object detection datasets. In: ECCV (2018)

- [9] Dwibedi, D., Misra, I., Hebert, M.: Cut, paste and learn: Surprisingly easy synthesis for instance detection. In: ICCV (2017)
- [10] Fan, D.P., Ji, G.P., Sun, G., Cheng, M.M., Shen, J., Shao, L.: Camouflaged object detection. In: CVPR (2020)
- [11] Fang, H.S., Sun, J., Wang, R., Gou, M., Li, Y.L., Lu, C.: Instaboost: Boosting instance segmentation via probability map guided copy-pasting. In: ICCV (October 2019)
- [12] Ghiasi, G., Cui, Y., Srinivas, A., Qian, R., Lin, T.Y., Cubuk, E.D., Le, Q.V., Zoph, B.: Simple copy-paste is a strong data augmentation method for instance segmentation. In: CVPR. pp. 2918–2928 (June 2021)
- [13] Girshick, R., Donahue, J., Darrell, T., Malik, J.: Rich feature hierarchies for accurate object detection and semantic segmentation. In: CVPR (2014)
- [14] Goodfellow, I.J., Pouget-Abadie, J., Mirza, M., Xu, B., Warde-Farley, D., Ozair, S., Courville, A., Bengio, Y.: Generative adversarial nets. In: NeurIPS. p. 2672–2680 (2014)
- [15] Hafiz, A.M., Bhat, G.M.: A survey on instance segmentation: state of the art. IJMIR **9** (2020)
- [16] He, K., Gkioxari, G., Dollár, P., Girshick, R.: Mask R-CNN. In: ICCV (2017)
- [17] Huang, Z., Huang, L., Gong, Y., Huang, C., Wang, X.: Mask Scoring R-CNN. In: CVPR (2019)
- [18] Jocher, G., Nishimura, K., Mineeva, T., Vilariño, R.: Yolov5. Code repository <https://github.com/ultralytics/yolov5> (2020)
- [19] Kirillov, A., Wu, Y., He, K., Girshick, R.: Pointrend: Image segmentation as rendering. In: CVPR (June 2020)
- [20] Le, T.N., Cao, Y., Nguyen, T.C., Le, M.Q., Nguyen, K.D., Do, T.T., Tran, M.T., Nguyen, T.V.: Camouflaged instance segmentation in-the-wild: Dataset, method, and benchmark suite. IEEE TIP (2021)
- [21] Le, T.N., Nguyen, T.V., Nie, Z., Tran, M.T., Sugimoto, A.: Anabranh network for camouflaged object segmentation. CVIU **184**, 45–56 (2019)
- [22] Le, T.N., Sugimoto, A., Ono, S., Kawasaki, H.: Attention r-cnn for accident detection. In: IEEE Intelligent Vehicles Symposium (2020)
- [23] Li, L., Rigall, E., Dong, J., Chen, G.: MAS3K: an open dataset for marine animal segmentation. In: BenchCouncil International Symposium on Benchmarking, Measuring, and Optimizing. pp. 194–212 (2020)
- [24] Lin, T.Y., Maire, M., Belongie, S., Hays, J., Perona, P., Ramanan, D., Dollár, P., Zitnick, C.L.: Microsoft coco: Common objects in context. In: ECCV (2014)
- [25] Liu, L., Ouyang, W., Wang, X., Fieguth, P.W., Chen, J., Liu, X., Pietikäinen, M.: Deep learning for generic object detection: A survey. IJCV **128** (2019)
- [26] Maekawa, T., Ohara, K., Zhang, Y., Fukutomi, M., Matsumoto, S., Matsumura, K., Shidara, H., Yamazaki, S.J., Fujisawa, R., Ide, K., Nagaya, N., Yamazaki, K., Koike, S., Miyatake, T., Kimura, K.D., Ogawa, H., Takahashi, S., Yoda, K.: Deep learning-assisted comparative analysis of animal trajectories with deephl. Nature Communications **11** (2020)
- [27] Mathis, M.W., Mathis, A.: Deep learning tools for the measurement of animal behavior in neuroscience. Current Opinion in Neurobiology **60**, 1–11 (2020)
- [28] Minaee, S., Boykov, Y.Y., Porikli, F., Plaza, A.J., Kehtarnavaz, N., Terzopoulos, D.: Image segmentation using deep learning: A survey. IEEE TPAMI (2021)

- [29] Nguyen, K.D., Nguyen, H.H., Le, T.N., Yamagishi, J., Echizen, I.: Effectiveness of detection-based and regression-based approaches for estimating mask-wearing ratio. In: *IEEE International Conference on Automatic Face and Gesture Recognition*. pp. 1–8 (2021)
- [30] Nguyen, V.T., Le, T.N., Bui, Q.M., Tran, M.T., Duong, A.D.: Smart shopping assistant: A multimedia and social media augmented system with mobile devices to enhance customers’ experience and interaction. In: *Pacific Asia Conference on Information Systems* (2012)
- [31] Parkhi, O.M., Vedaldi, A., Zisserman, A., Jawahar, C.V.: Cats and dogs. In: *CVPR* (2012)
- [32] Qiao, S., Wang, H., Liu, C., Shen, W., Yuille, A.: Weight standardization. *arXiv preprint arXiv:1903.10520* (2019)
- [33] Ren, S., He, K., Girshick, R., Sun, J.: Faster r-cnn: Towards real-time object detection with region proposal networks. In: *NeurIPS* (2015)
- [34] Rossi, L., Karimi, A., Prati, A.: A novel region of interest extraction layer for instance segmentation. *ICPR* (2021)
- [35] Shorten, C., Khoshgoftaar, T.: A survey on image data augmentation for deep learning. *Journal of Big Data* **6** (2019)
- [36] Solovyev, R., Wang, W., Gabruseva, T.: Weighted boxes fusion: Ensembling boxes from different object detection models. *Image and Vision Computing* **107**, 104117 (2021)
- [37] Szegedy, C., Liu, W., Jia, Y., Sermanet, P., Reed, S.E., Anguelov, D., Erhan, D., Vanhoucke, V., Rabinovich, A.: Going deeper with convolutions. In: *CVPR* (2015)
- [38] Takahashi, R., Matsubara, T., Uehara, K.: Data augmentation using random image cropping and patching for deep cnns. *IEEE TCSVT* **30**(9) (2020)
- [39] Tran, M.T., Nguyen, T.V., Hoang, T.H., Le, T.N., Nguyen, K.T., Dinh, D.T., Nguyen, T.A., Nguyen, H.D., Nguyen, T.T., Hoang, X.N., Vo-Ho, V.K., Do, T.L., Nguyen, L., Le, M.Q., Nguyen-Dinh, H.P., Pham, T.T., Nguyen, X.V., Nguyen, E.R., Tran, Q.C., Tran, H., Dao, H., Tran, M.K., Nguyen, Q.T., Vu-Le, T.A., Nguyen, T.P., Diep, G.H., Do, M.N.: itask - intelligent traffic analysis software kit. In: *CVPR Workshops* (2020)
- [40] Vo, D.M., Le, T.N., Sugimoto, A.: Balancing content and style with two-stream fcns for style transfer. In: *WACV* (2018)
- [41] Wah, C., Branson, S., Welinder, P., Perona, P., Belongie, S.: The Caltech-UCSD Birds-200-2011 dataset. Tech. Rep. CNS-TR-2011-001, California Institute of Technology (2011)
- [42] Wang, J., Chen, K., Xu, R., Liu, Z., Loy, C.C., Lin, D.: Carafe: Content-aware reassembly of features. In: *ICCV* (October 2019)
- [43] Wu, X., Zhan, C., Lai, Y., Cheng, M.M., Yang, J.: IP102: A large-scale benchmark dataset for insect pest recognition. In: *CVPR* (2019)
- [44] Wu, Y., He, K.: Group normalization. In: *ECCV* (2018)
- [45] Yun, S., Han, D., Oh, S.J., Chun, S., Choe, J., Yoo, Y.: CutMix: Regularization strategy to train strong classifiers with localizable features. In: *ICCV* (2019)
- [46] Zhang, H., Cisse, M., Dauphin, Y.N., Lopez-Paz, D.: mixup: Beyond empirical risk minimization. In: *ICLR* (2018)
- [47] Zhu, X., Hu, H., Lin, S., Dai, J.: Deformable convnets v2: More deformable, better results. *CVPR* (2019)